

Photophysical Study of Blue, Green, and Orange-Red Light-Emitting Carbazoles¹

Ravi M. Adhikari and Douglas C. Neckers*

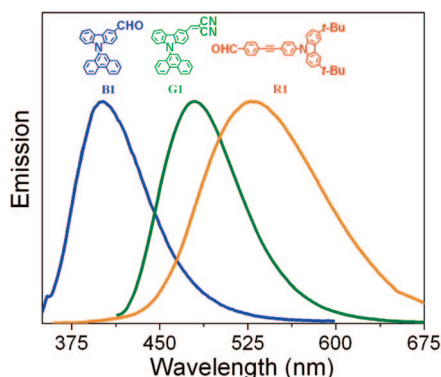
Center for Photochemical Sciences, Bowling Green State University, Bowling Green, Ohio 43402

Bipin K. Shah*

Department of Chemistry, Pittsburg State University, Pittsburg, Kansas 66762

bshah@pittstate.edu; neckers@photo.bgsu.edu

Received February 6, 2009



Simple synthetic procedures have been developed to prepare suitably substituted stable carbazoles **B1–B3**, **G1–G3**, and **R1–R3**. These compounds emit blue, green, and orange-red light, respectively, and show a red-shifted emission in the solid state relative to that in solution. The extent of the shift is highly dependent on the nature and the positions of the substituents. A red-shift as high as 120 nm can be achieved by a suitable substitution, especially by N-substitution of carbazole. The presence of a carbaldehyde or malononitrile group on the carbazole moiety is found to quench fluorescence severely in solution and in the solid state, as indicated by low fluorescence quantum yields of **B1** ($\phi_F \sim 0.03$), **B3** ($\phi_F \sim 0.04$), and **G1–G3** ($\phi_F \sim 0.04–0.15$). However, the effect is not the same for the fluorescence lifetime ($\tau_F \sim 1–5.69$ ns). The rate constants of radiative and nonradiative deactivation of **B1–R3** have been found to be in the range of 6.40×10^6 to 9.50×10^8 and 1.38×10^8 to 9.84×10^8 , respectively. Lowering the temperature from 25 to -10 °C causes a small but distinct red-shift in the emissions and a systematic increase in the ϕ_F values of the blue and green emitters. Solvatochromism and concentration-dependent emissions of the compounds are also discussed.

Introduction

The application of organic electroluminescent materials in flat-panel displays has led to an intensive search for stable organic materials that can emit light with high efficiency and brightness.^{2–7} A set of pure red, green, and blue emitters is required for full-color displays. Carbazoles are known for intense luminescence and are widely used in organic light-emitting diodes (OLEDs) as blue, green, red, and white emitters.^{8–19}

They also undergo reversible oxidation processes that makes them suitable hole carriers.^{20–22} The molecular and optical properties of carbazole can be tuned by structurally modifying its 2, 3, 6, 7, and 9H positions.^{23–25} In fact, the light-emitting property combined with the hole-transporting capability of

(1) Contribution no. 739 from the Center for Photochemical Sciences.
 (2) Tang, C. W.; VanSlyke, S. A. *Appl. Phys. Lett.* **1987**, *51*, 913.

(3) Shinar, J. *Organic Light-Emitting Devices*; Springer-Verlag: New York, 2003.

(4) *Organic Light-Emitting Devices. Synthesis Properties and Applications*; Mullen, K., Scherf, U., Eds.; Wiley-VCH Verlag GmbH & Co. KGaA: Weinheim, Germany, 2006.

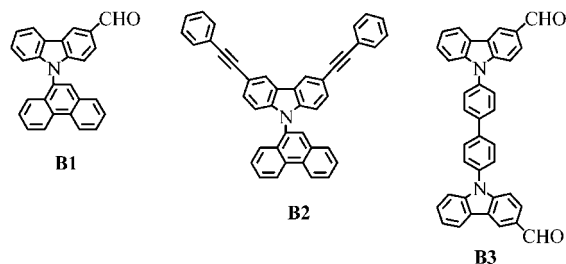
(5) Yu, M.-X.; Chang, L.-C.; Lin, C.-H.; Duan, J.-P.; Wu, F.-I.; Chen, I.-C.; Cheng, C.-H. *Adv. Funct. Mater.* **2007**, *17*, 369.

carbazoles make them one of the important classes of compounds that have been actively pursued for applications in OLEDs and other optoelectronic devices.

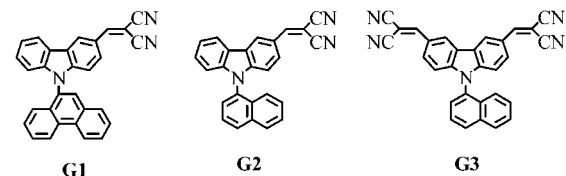
Although studies on carbazoles have appeared in the literature over the past few years, they are mostly focused on their use as materials and applications in devices.^{8–22} We have developed a new series of carbazoles (Figure 1, **B1–B3**, **G1–G3**, and **R1–R3**) that exhibit stable blue, green, and orange-red emission in solution and in the solid state. This prompted a systematic study of **B1–B3**, **G1–G3**, and **R1–R3** in an attempt to understand the photophysical properties and structure–property relationships in these compounds. While **B1** and **B3** each possess mild electron-withdrawing (EW) carbaldehyde groups, **B2** lacks such a group. Compounds **G1–G3** and **R2–R3** are substituted with strong EW malononitrile groups at various positions. It was observed that the effect of the extension of conjugation on the emission is more profound when an appropriate substituent is at the N-position than at the 3 and 6 positions. We also report on the solvatochromic properties, concentration-dependent fluorescence switching, and the temperature-dependent fluorescent behavior of these new systematically substituted carbazoles.

Compounds **B1–B3** emit intense blue light both in solution and in the solid state, while compounds containing the malononitrile group attached to the carbazole moiety (**G1–G3**) show green emission. It is interesting that **R1**, which is the immediate synthetic precursor of **R2**, shows an orange emission in solution but a bluish-green emission in the solid state, whereas **R2** emits orange in solution and almost red in the solid state. On the other hand, **R3** shows a green emission in dichloromethane and orange-red in the thin film. Moreover, **R2** and **R3** are rather different from **B1–B3**, **G1–G3**, and **R1** in that the former compounds readily form nanoparticles under our now well-defined tetrahydrofuran(THF)/water system and their emission can be switched on and off by manipulating the THF/water ratio.²⁶ However, the latter compounds show no such behavior.

(A) Blue emitters



(B) Green emitters



(C) Red emitters

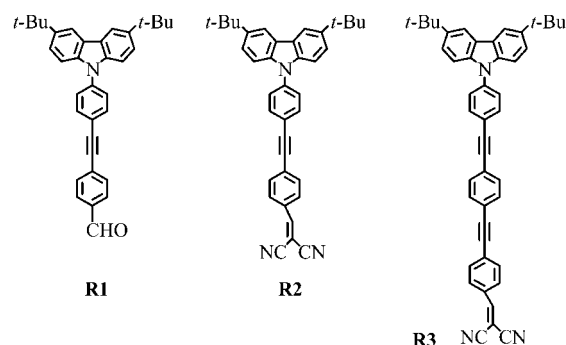


FIGURE 1. Structure of blue-, green-, and red-emitting carbazoles.

Results and Discussion

Synthesis. Compounds **B1–B3** were synthesized starting from carbazole (**1**) (Scheme 1). The first step involved N-substitution of **1** by the naphthyl and phenanthryl groups resulting in **2** and **3**, respectively. Bromination and iodination of **2** and **3** at the 3 and 6 positions provided **4–6**. Compound **4** was treated with *n*-butyllithium and dimethylformamide resulting in **B1**. Sonogashira coupling of **5** with phenylacetylene proved to be a difficult reaction. Thus, iodo-substituted **6** was synthesized, and this easily yielded **B2**. The reaction of **1** with 4,4'-dibromobiphenyl (**7**) in the presence of potassium carbonate yielded **8**. Formylation of the latter introduces the aldehydic functionalities at the 3 and 3' positions of carbazole, forming **B3**.

Reaction of either of **4** and **5** with BuLi and DMF in ether (formylation) resulted in a mixture of mono- and diformylated products (Scheme 2) that were separated using column chromatography. Treatment of monoformylated products (**9** and **B1**) with malononitrile and basic aluminum oxide in toluene produced **G1** and **G2**, respectively. A similar reaction of 3,6-diformylated *N*-naphthyl product (**10**) yielded **G3**. The syntheses of **R1–R3** are described elsewhere.²⁶

Absorption and Emission Spectra in Solution. Representative examples of the absorption and emission spectra recorded in dichloromethane are shown in Figures 2 and 3, respectively.

(6) Shah, B. K.; Neckers, D. C.; Shi, J.; Forsythe, E. W.; Morton, D. J. *Phys. Chem. A* **2005**, *109*, 7677.

(7) Thomas, K. R.; Lin, J. T.; Tao, Y. T.; Ko, C. *J. Am. Chem. Soc.* **2001**, *123*, 9404.

(8) Yu, H.; Zain, S. M.; Eigenbrot, I. V.; Phillips, D. *Chem. Phys. Lett.* **1993**, *202*, 141.

(9) Howell, R.; Taylor, A. G.; Phillips, D. *Chem. Phys. Lett.* **1992**, *188*, 119.

(10) Almeida, K. D.; Bernede, J. C.; Marsillac, S.; Godoy, A.; Diaz, F. R. *Synth. Met.* **2001**, *122*, 127.

(11) Lee, J.; Woo, H.; Kim, T.; Park, W. *Opt. Mater.* **2002**, *21*, 225.

(12) Ding, J.; Gao, J.; Cheng, Y.; Xie, Z.; Wang, L.; Ma, D.; Jing, X.; Wang, F. *Adv. Funct. Mater.* **2006**, *16*, 575.

(13) Morin, J.; Boudreault, P.; Leclerc, M. *Macromol. Rapid Commun.* **2002**, *23*, 1032.

(14) Grigalevicius, S.; Ma, L.; Xie, Z.; Scheri, U. *J. Polym. Sci., Part A: Polym. Chem.* **2006**, *44*, 598713.

(15) Liu, Y.; Nishiura, M.; Wang, Y.; Hou, Z. *J. Am. Chem. Soc.* **2006**, *128*, 5592.

(16) Guan, M.; Chen, Z.; Bian, Z.; Liu, Z.; Gong, G.; Baik, W.; Lee, H.; Huang, C. *Org. Electron.* **2006**, *7*, 330.

(17) Adhikari, R. M.; Mondal, R.; Shah, B. K.; Neckers, D. C. *J. Org. Chem.* **2007**, *72*, 4727.

(18) Yu, M.-X.; Chang, L.-C.; Lin, C.-H.; Duan, J.-P.; Wu, F.-I.; Chen, I.-C.; Cheng, C.-H. *Adv. Funct. Mater.* **2007**, *17*, 369.

(19) Zhao, Z.; Li, J.-H.; Chen, X.; Wang, X.; Lu, P.; Yang, Y. *J. Org. Chem.* **2009**, *74*, 383.

(20) Loiseau, F.; Campagna, S.; Hameurlaine, A.; Dehaen, W. *J. Am. Chem. Soc.* **2005**, *127*, 11352.

(21) Jiang, X.; Register, R. A.; Richard, A.; Killen, K. A.; Thompson, M. E.; Pschenitzka, F.; Sturm, J. C. *Chem. Mater.* **2000**, *12*, 2542.

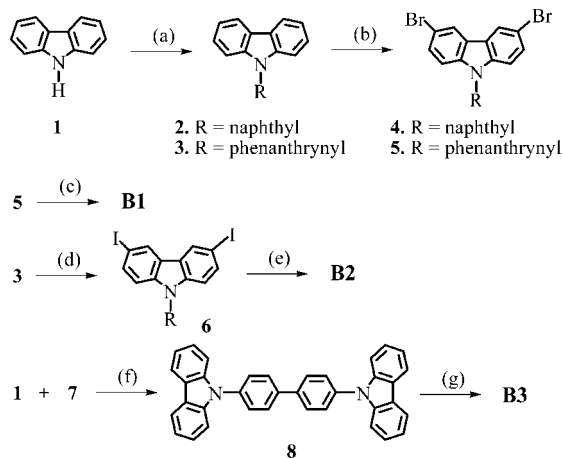
(22) Tao, Y.; Wang, Q.; Yang, C.; Wang, Q.; Zhang, Z.; Zou, T.; Qin, J.; Ma, D. *Angew. Chem., Int. Ed.* **2008**, *47*, 8104.

(23) Joule, J. A. *Adv. Heterocycl. Chem.* **1984**, *35*, 83.

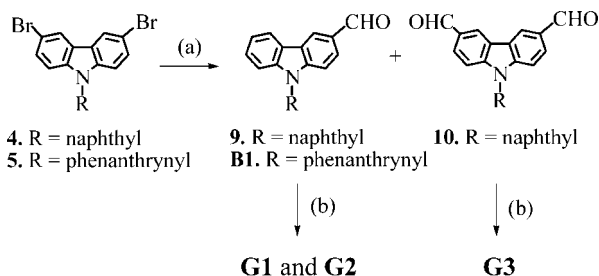
(24) Zhu, Z.; Moore, J. S. *J. Org. Chem.* **2000**, *65*, 116.

(25) Zhu, Z.; Moore, J. S. *Macromolecules* **2000**, *33*, 801.

(26) Adhikari, R. M.; Shah, B. K.; Palayangoda, S. S.; Neckers, D. C. *Langmuir* **2009**, *25*, 2402.

SCHEME 1. Synthesis of B1–B3^a

^a Reactions and conditions: (a) 1-bromonaphthalene or 9-bromophenanthrene, K₂CO₃, nitrobenzene, reflux 48 h; (b) *N*-bromosuccinimide, dichloromethane; (c) *n*-BuLi, ether, DMF, -70 °C; (d) *N*-iodosuccinimide, dichloromethane; (e) phenylacetylene, Pd(PPh₃)₂Cl₂, CuI, PPh₃, triethylamine, reflux 12 h; (f) 4-4'-dibromobiphenyl (7), K₂CO₃, nitrobenzene, reflux 3 days; (g) POCl₃, DMF, 1,2-dichloroethane, reflux 12 h.

SCHEME 2. Synthesis of G1–G3^a

^a Reactions and conditions: (a) *n*-BuLi, DMF, ether, -70 °C; (b) malononitrile, toluene, basic Al₂O₃, reflux 6 h.

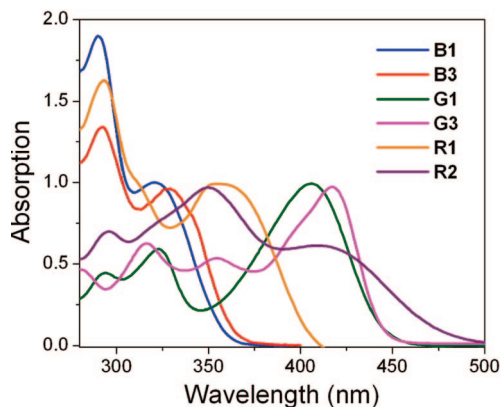


FIGURE 2. Absorption spectra of B1, B3, G1, G3, R1, and R2 recorded in dichloromethane.

The absorptions of compounds that have a weak EW group (B1, B3, and R1) or no EW group (B2) are similar to that of carbazole, each comprising two absorption maxima ($\lambda_{\max} \sim 290$ nm and $\lambda_{\max} \sim 320$ –350 nm). The latter absorption can be assigned to the π - π^* transition. The absorptions of G1–G3 and R2–R3 are different in that each of them shows an additional absorption maximum. The low energy absorption ($\lambda_{\max} \sim 380$ –420 nm) of G1–G3 and R2–R3 can be assigned to an intramolecular charge-transfer (ICT) transition.^{18,26,27} In other words, formation of the ICT state was not observed in

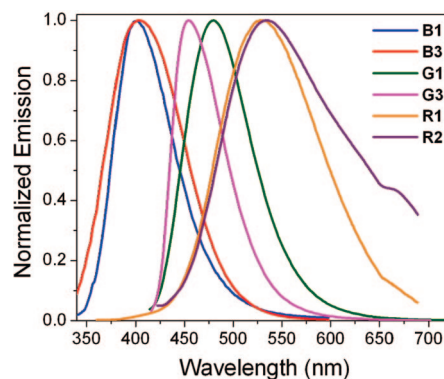


FIGURE 3. Normalized emission spectra of B1, B3, G1, G3, R1, and R2 recorded in dichloromethane.

B1–B3 and R1. The low energy absorption band in G1–G3 and R1–R3 underwent a small but gradual red-shift when solvents of increasing polarity were used (see Supporting Information). This further supports the assignment of the low energy band to the ICT transition in these molecules. An ICT state is expected to be more stable in polar solvents. On the other hand, the high energy absorption bands showed no dependency on the solvent polarity. The extinction coefficients (ϵ) of absorption at the peak corresponding to the π - π^* transition were in the range of 12 500–48 000 L mol⁻¹ cm⁻¹, except for G2 and G3. The ϵ values of the latter compounds (293 000 and 110 000 L mol⁻¹ cm⁻¹, respectively) were much higher.

The emission spectra of B1–B3, G1–G3, and R1–R3 recorded in dichloromethane extend from the violet-blue to orange-red regions. The samples were excited at wavelengths corresponding to the π - π^* transition to make sure that the emission originated from the singlet excited state. One would assume that the presence of the ethynylphenyl groups *para* to nitrogen in carbazole should increase the effective conjugation length in the molecule. Nevertheless, the emission maxima of B1–B3 ($\lambda_{\max} = 392$ –405 nm) were similar, indicating that substitution of carbazole with either a smaller carbaldehyde group or conjugation-extending ethynylphenyl groups at the 3 and 6 positions causes no significant red-shift. It may be possible that excitation to the S₁ state is principally located at the nitrogen atom in the carbazole moiety in these molecules. In other words, the electronic density concentrated around nitrogen contributes significantly more to the HOMO and LUMO orbitals than that around the carbon atoms at 3 and 6 positions.

The geometry optimized structures of B1 and B2 show the phenanthrynyl group almost orthogonal to the carbazole moiety (Supporting Information). Interestingly, even though the ethynylphenyl group and the carbazole moiety are coplanar in B2, its emission ($\lambda_{\max} = 392$ nm) is not red-shifted significantly relative to that of B1 ($\lambda_{\max} = 402$ nm). This reinforces that extension of conjugation due to the ethynylphenyl groups at the 3 and 6 positions imparts a negligible effect on the emission. Nevertheless, N-substitution by the ethynylphenyl group that contains an aldehydic or malononitrile group causes a large red-shift in the emission (*vide infra*). This suggests that the extent of electron delocalization through the 9 position in carbazoles is significantly higher than that through the 3 or 6 positions. This is similar to the observations that electron transfer is more

(27) Nikolaev, A. E.; Myszkiewicz, G.; Berden, G.; Meerts, W. L.; Pfanstiel, J. F.; Pratt, D. W. *J. Chem. Phys.* **2005**, *122*, 84309.

TABLE 1. Photophysical Properties of B1–B3, G1–G3, and R1–R3 Recorded in Dichloromethane and in Thin Films^a

compound	solution						solid	
	A_{\max} (nm)	λ_{\max} (nm)	τ_F (ns)	ϕ_F	$k_R^0 \cdot 10^{-7}$ (s ⁻¹)	$k_{NR}^0 \cdot 10^{-8}$ (s ⁻¹)	λ_{\max} (nm)	ϕ_F
B1	290, 321	402	4.68	0.03 ± 0.01	0.64	2.06	418	0.04 ± 0.01
B2	299, 330	392	4.27	0.32 ± 0.03	10.5	2.23	400	0.45 ± 0.06
B3	292, 329	405	~1	0.04 ± 0.01	4.10	9.84	418	0.06 ± 0.01
G1	294, 323, 406	480	4.68	0.04 ± 0.01	0.85	2.04	515	0.11 ± 0.02
G2	292, 321, 404	473	<1	0.05 ± 0.01	5.00	9.50	502	0.12 ± 0.02
G3	316, 356, 418	453	<1	0.07 ± 0.01	7.00	9.30	525	0.15 ± 0.02
R1	293, 354	528	5.69	0.10 ± 0.01	1.78	1.60	445	0.21 ± 0.03
R2	296, 350, 410	534	4.20	0.40 ± 0.03	9.50	1.42	600	0.34 ± 0.05
R3	350, 382	474	3.70	0.30 ± 0.02	8.10	1.80	594	0.25 ± 0.04

^a Compounds were excited at the corresponding A_{\max} representing the $\pi-\pi^*$ transition for τ_F and ϕ_F . The ϕ_F and τ_F values were measured from argon-saturated solutions, and decay was monitored at the corresponding λ_{\max} . The optical density of the samples for τ_F and ϕ_F measurements were less than 0.13 and 0.09, respectively. The ϕ_F values for **B1–B3** and **G1–G3** are relative to that of diphenylanthracene (0.90 in cyclohexane). The ϕ_F values for **R1–R3** are relative to that of riboflavin (0.3 in ethanol).

efficient when an electron-accepting group is linked to nitrogen (9 position) in carbazoles.^{28,29}

Significant differences were observed in the fluorescence quantum yields (ϕ_F) of **B1–B3** (Table 1). The ϕ_F values of **B1** (0.03) and **B3** (0.04) were smaller by an order of magnitude than that of **B2** (0.32). Carbaldehyde substitution significantly decreases the fluorescence quantum yield. Since there is no ICT complex forming in **B1–B3**, the quenching of the fluorescence cannot be attributed to a charge transfer process. This may be related with intramolecular electron transfer or free bond rotation around C–CHO causing excitation diffusion and deactivation.³⁰ In other words, rotational deactivation increases the chance of nonradiative relaxation of the excited singlet state, resulting in the decrease in the ϕ_F value. The effect of the carbaldehyde group on the fluorescence lifetime (τ_F) was not the same. Although the τ_F value of **B3** (1 ns) was abnormally short, the τ_F value of **B1** (4.68 ns) was found to be similar to that of **B2** (4.27 ns).

The difference in the structure of **B1** and **G1** is that the latter contains a malononitrile group instead of a carbaldehyde group (Figure 1). However, the emission of **G1** ($\lambda_{\max} = 480$ nm) was red-shifted by about 80 nm relative to that of **B1** ($\lambda_{\max} = 402$ nm). As pointed out above, the additional conjugation provided by the malononitrile groups in **G1** does not account for such a significant red-shift in the emission. If this were the case, the emission of **G3** would have been red-shifted in comparison to that of **G2** because the former contains one malononitrile group, whereas the latter has two such groups. Since both malononitrile groups are in conjugation with nitrogen of carbazole, the electronic propensity of the carbazole nucleus should have extended more in **G3** than in **G2**. In contrast, the emission of **G3** ($\lambda_{\max} = 454$ nm) is actually blue-shifted relative to that of **G2** ($\lambda_{\max} = 473$ nm).

The effect of the malononitrile group in causing a blue-shift in the emission is probably associated with its ability to influence the polarity of the excited singlet state. This is also supported by the strong solvatochromic effect observed in these compounds (vide infra). The singlet states of **G1** and **G2** are less polar than that of **G3** due to the presence of two EW malononitrile groups in the latter.³¹ A highly polar singlet state would be less stabilized in relatively nonpolar dichloromethane,

causing a blue-shifted emission from **G3**. It is also likely that the order of the emission wavelength (**G1** > **G2** > **G3**) is related with the propensity of the ICT complex of these molecules. For example, since **G1** has a better electron-donating group (phenanthryl) than **G2** and **G3** (naphthyl), the propensity of the ICT complex may be higher in **G1** than in **G2**. Although the phenanthryl and naphthyl groups are almost orthogonal to the carbazole moiety, these groups do contribute to the electronic density of the carbazole nucleus.

The malononitrile group also causes a significant decrease in the fluorescence quantum efficiencies similar to the carbaldehyde group. The ϕ_F values of **G1–G3** (0.04–0.07) were found to be much lower than that of carbazole (0.42).³² Thus, these compounds exhibit a behavior similar to that of other systems where quenching of fluorescence has been observed to be caused by EW groups such as the cyano group.^{33,34} The effect of the malononitrile group on the fluorescence lifetime (τ_F) was, however, not similar. Compounds **G2** and **G3** exhibited abnormally short lifetime τ_F (<1 ns), while that of **G1** was ~4.68 ns.

We have earlier shown that *N*-phenylethynylphenyl-substituted carbazoles exhibit an intense blue emission in dichloromethane.¹⁷ However, the presence of a carbaldehyde or malononitrile substituent on the *N*-ethynylphenyl group completely changes the emission behavior, as exhibited by the large red-shifted emission of **R1** and **R2**. For example, **R1** ($\lambda_{\max} = 528$ nm) and **R2** ($\lambda_{\max} = 534$ nm) emit orange light in dichloromethane, whereas 3,6-di-*tert*-butyl-9-(4-(2-phenylethynyl)phenyl)-9*H*-carbazole, an analogue of **R1** and **R2** without the carbaldehyde or the malononitrile group, emits blue ($\lambda_{\max} = 410$ nm).¹⁷ The emission behavior of **R3** is more interesting. It emits bluish-green light ($\lambda_{\max} \sim 474$ nm) in dichloromethane, although it contains an additional ethynylphenyl group relative to **R1** and **R2**. The emission maximum of **R3** is blue-shifted about 55–65 nm relative to those of **R1** and **R2**. The emission of **R2** originating from the ICT state and that of **R3** originating from the singlet excited state does not appear to be the reason.

(31) The free rotation of the C–C single bond between the phenyl and the two malononitrile groups in **G3** allows the latter to alternately come close together and go far away from each other. Such a rotation may lead to a higher resultant dipole in the ground state of **G3** than in the ground state of **G2**, which has only one malononitrile group. The order of the dipole in the ground state may be retained in the singlet excited states of these compounds.

(32) *Handbook of Organic Photochemistry*; Scaiano, J. C., Ed.; CRC Press: Boca Raton, FL, 1989; Vol. 1, p 22.

(33) Michel, B.; Jean-Francois, M.; Mario, L.; Gilles, D. *J. Phys. Chem. A* **2005**, *109*, 6953.

(34) Li, C.-L.; Shieh, S.-J.; Lin, S.-C.; Liu, R.-S. *Org. Lett.* **2003**, *5*, 1131.

(28) Zotti, G.; Schiavon, G.; Zecchin, S.; Morin, J.-F.; Leclerc, M. *Macromolecules* **2002**, *35*, 2122.

(29) Kapturkiewicz, A.; Herbich, J.; Karpiuk, J.; Npwacki, J. *J. Phys. Chem. A* **1997**, *101*, 2332.

(30) Lakowicz, J. R. *Principles of Fluorescence Spectroscopy*; Springer: New York, NY, 2006; p 278.

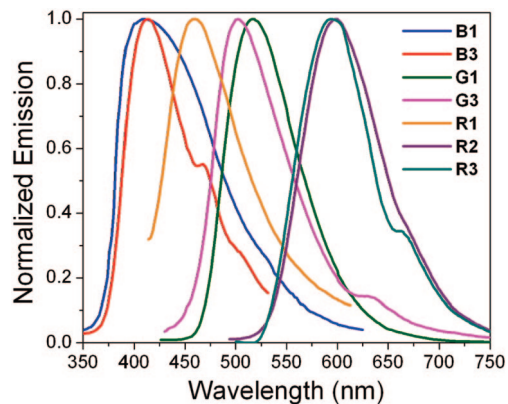


FIGURE 4. Normalized emission spectra of thin films of **B1**, **B3**, **G1**, **G3**, and **R1–R3**.

If this were the case, the emission of **R1** would not have been highly red-shifted because there is no formation of the ICT state in **R1**.

The additional ethynylphenyl group in **R3** should increase its rotational flexibility. However, the geometry optimized structure of **R3** shows that the long 1,4-diethynylphenylbenzene side chain is flat in this molecule. Thus, it may be that the overall molecular rigidity increases in **R3** compared to that in **R1** or **R2** due to the additional ethynylphenyl group, which may be the cause of the blue-shifted emission of the former. Nonetheless, less communication between the carbazole moiety and the diethynylphenylbenzene side chain and both behaving as separate chromophoric units in **R3** appears to be a more reasonable explanation. The blue-greenish emission of **R3** is broader than that of **R1** and **R2** and may have contribution from both chromophoric units. The observation of two distinct fluorescence lifetimes in the case of **R3** further supports this explanation (vide infra). It is also noted that the absorption of **R3** is structureless and much broader than those of **B1–B3**, **G1–G3**, or **R1–R2** (see Supporting Information).

The ϕ_F values of **R1** (~ 0.10), **R2** (~ 0.40), and **R3** (~ 0.30) were found to be larger than those of **G1–G3** ($\sim 0.04–0.07$). Compound **R1** showed a longer τ_F (5.69 ns) compared to those of **R2** ($\tau_F \sim 4.20$ ns) and **R3** ($\tau_F \sim 3.70$ ns). In fact, the fluorescence decays of **R1–R3** were biexponential, whereas those of **B1–B3** or **G1–G3** were monoexponential. However, the lifetimes of the shorter components of **R1** and **R2** were observed to be too low (<1 ns) and close to the instrument response time to have any physical significance. The two distinct lifetimes (1.80 and 3.70 ns) observed in the case of **R3** are most probably due to two separate singlet states associated with the carbazole and 1,4-diethynylphenylbenzene moieties. It should be noted that there is no systematic difference in the rate constants of radiative deactivation (k_R^0) of the three classes of compounds. For example, the k_R^0 values of **B1–B3** ($\sim 6.40 \times 10^6$ to 1.49×10^8 s $^{-1}$), **G1–G3** ($\sim 8.54 \times 10^6$ to 7.00×10^7 s $^{-1}$), and **R1–R3** ($\sim 1.78 \times 10^6$ to 9.50×10^8) are in the same range, although the difference between individual compounds is as high as 2 orders of magnitude.

Emission in the Solid State. The emissions of all compounds except **R1** in the solid state were found to be red-shifted compared to the corresponding emission in solution (Figure 4). This is most probably due to molecular stacking in the solid state. Solid-state packing has, however, little effect on the shape of the emission because the thin film emissions of each were similar to the corresponding emissions in dichloromethane. The

red-shift in solid-state emission results from interaction of neighboring polar substituents since the compounds are more polar in the singlet excited states than in the ground states (vide infra). Intermolecular interaction of neighboring polar substituents lowers the energy level of the excited states. This also explains why the extent of the red-shift was smaller for **B1–B3** (8–16 nm), which have either weak or no EW substituents.

Compounds **G1–G3** contain more polar malonitrile groups and exhibit a moderate red-shift (~ 30 nm). The red-shift was large in the cases of **R2** (66 nm) and **R3** (120 nm). On the other hand, **R1** is strikingly different in that its emission showed a blue-shift of ~ 85 nm, even though the structures of **R1** and **R2** are similar. The replacement of the carbaldehyde group in **R1** ($\lambda_{\max} = 445$ nm) with a malonitrile group **R2** ($\lambda_{\max} = 600$ nm) does not electronically account for the emission difference in the solid state. However, it is possible that these groups may induce formation of different types of aggregates in the solid state. Since **R2** is more polar than **R1**, the different aggregate formation is likely due to their different dipole moments. Compound **R1** probably forms H-aggregates in the solid state resulting in a blue-shift, whereas **R2** undergoes J-aggregation that accounts for the red-shift.^{35,36}

The solid-state emission behavior of **R3** seems interestingly different and needs special mention. There is no apparent difference in the structure of **R2** and **R3**, except that the latter contains an additional ethynylphenyl group, but the red-shift observed in the case of **R3** (120 nm) is almost double that observed in the case of **R2** (66 nm). The huge red-shift in the solid-state emission of **R3** is partly due to the fact that the solution absorption of **R3** is significantly blue-shifted compared to that of **R2**. Nonetheless, it is clear that emissions in solution and in the solid state are from different excited states of **R3**. It appears that **R3** in solution emits from the $\pi-\pi^*$ state of the discrete carbazole moiety and the phenylethynylphenyl side chain (vide supra), but from the ICT state in the solid state. It is also possible that, while both **R2** and **R3** probably form J-aggregates in the solid state, the latter may be more closely stacked. The presence of the additional ethynyl group and the longer flat portion of the molecule provide a possibility of greater intermolecular π -interaction in the molecules of **R3**, resulting in highly red-shifted emission in the solid state. It is unfortunate that we could not obtain crystal structures of these compounds because of their amorphous nature and cannot comment on the exact nature of the molecular stacking in the solid state.

All of these compounds, except for **G3**, exhibit an excimer emission. Very weak excimer emission was observed in the case of **G3** (630 nm). The ϕ_F values of **B1–R3** in the solid state were found similar to the corresponding values observed in dichloromethane (Table 1). The ϕ_F values of **B2** (0.45) and **R1–R3** (0.21–0.34) were reasonable, but **B1**, **B3**, and **G1–G3** showed very low ϕ_F values ($<15\%$), indicating that the presence of the carbaldehyde or the malonitrile group on the carbazole moiety severely quenches the fluorescence. However, the ϕ_F values of **R1–R3** (0.21–0.34) suggest that the presence of these groups on the side ethynylphenyl function fails to quench fluorescence in the solid state.

Solvatochromism. A solvatochromic effect was observed for those compounds (**B1**, **B3**, and **G1–G3**) that contain EW groups

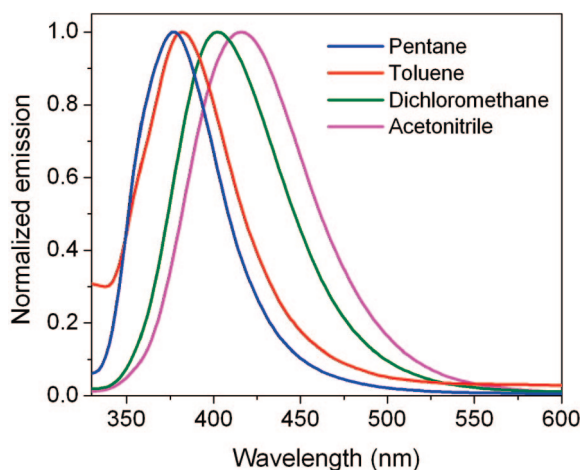
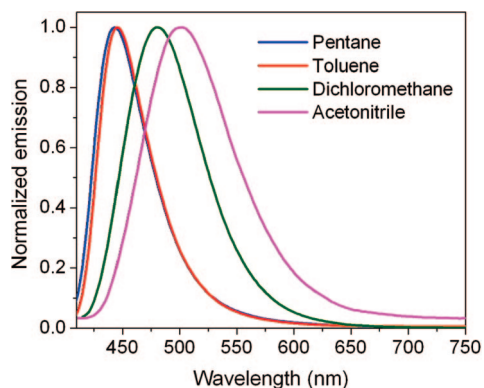
(35) Palayangoda, S. S.; Cai, C.; Adhikari, R. M.; Neckers, D. C. *Org. Lett.* **2008**, *10*, 281.

(36) Oelkrug, D.; Tompert, A.; Gierschner, J.; Egelhaaf, H.-J.; Hanack, M.; Hohloch, M.; Steinhuber, E. *J. Phys. Chem. B* **1998**, *102*, 1902.

TABLE 2. Absorption Maxima (A_{\max}), Emission Maxima (λ_{\max}), and Fluorescence Quantum Yields (ϕ_F) of **B1**, **G1**, and **R2** Measured in Different Solvents^a

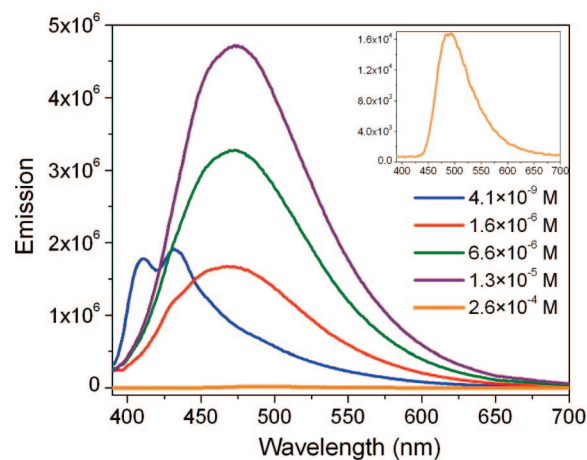
solvent	B1			G1			R2		
	A_{\max} (nm)	λ_{\max} (nm)	ϕ_F	A_{\max} (nm)	λ_{\max} (nm)	ϕ_F	A_{\max} (nm)	λ_{\max} (nm)	ϕ_F
pentane	313	376	0.025	393	451	0.16	345	448	0.50
toluene	316	380	0.022	402	445	0.16	348	554	0.48
dichloromethane	320	402	0.020	405	481	0.11	350	535	0.40
acetonitrile	314	416	0.015	395	503	0.09	346	490	0.33

^a Excitation wavelengths: **B1**, $\lambda_{\text{ex}} = 320$ nm; **G1**, $\lambda_{\text{ex}} = 320$ nm; and **R2**, $\lambda_{\text{ex}} = 350$ nm.

**FIGURE 5.** Normalized emission spectra of **B1** recorded in different solvents.**FIGURE 6.** Normalized emission spectra of **G1** recorded in different solvents.

on the carbazole. However, the effect was moderate, again suggesting that the EW groups at the 3 and 6 positions are not significantly involved in intermolecular charge distribution in the excited state. Representative examples of normalized fluorescence of **B1** and **G1** recorded in hexanes, toluene, dichloromethane, and acetonitrile are shown in Figures 5 and 6. The emission maxima were gradually red-shifted when the compounds were dissolved in the nonpolar pentane to the polar acetonitrile. The ground states of these compounds are polar due to varying degrees of charge separation in these molecules. It is clear that the singlet excited states are more polar than the ground states. The increased polarity of the singlet states stems from further charge separation following excitation. This solvatochromic effect is attributed to the decrease of the singlet excited-state energy with the increases of the solvent polarity.

It is noted that the extent of the red-shift from pentane to acetonitrile is almost similar for **B1** (40 nm) and **G1** (52 nm), although the latter contains a more polar group than the former

**FIGURE 7.** Emission spectra of **R3** recorded in dichloromethane at different concentrations ($\lambda_{\text{ex}} = 380$ nm). Inset: enlarged spectrum for the concentration of 2.6×10^{-4} M, which appears as a straight line in the main figure.

(Table 2). Nonetheless, the presence of the EW groups does account for the solvatochromic effect shown by these compounds. Compound **B2** with no EW group shows no significant solvatochromism (see Supporting Information). The emission maximum of **B2** in pentane ($\lambda_{\max} = 386$ nm), for example, is similar to that observed in acetonitrile ($\lambda_{\max} = 390$ nm). The cases of **R1–R3** were different, and a systematic solvatochromic effect was not observed for these compounds. Interestingly, **R2** shows a negative solvatochromic effect from toluene to dichloromethane ($\lambda_{\max} = 535$ nm) and acetonitrile ($\lambda_{\max} = 490$ nm), although it shows a large red-shift from pentane ($\lambda_{\max} = 448$ nm) to toluene ($\lambda_{\max} = 554$ nm). Such a behavior of **R1–R3** is probably due to formation of a twisted ICT in their excited singlet states.^{18,27} N-Substituted carbazoles that have an elongated structure similar to that of **R1–R3** are known to form twisted ICT excited states that behave differently in different solvents.^{18,27}

The ϕ_F values of **B1**, **G1**, and **R2**, three representative examples, are included in Table 2. The ϕ_F values decrease slightly going from a nonpolar to a polar solvent. The ϕ_F value of **B1** in pentane (0.025), for example, was slightly higher than that in acetonitrile (0.015). Similarly, the ϕ_F value of **R2** decreased from 0.50 in pentane to 0.33 in acetonitrile.

Concentration-Dependent Fluorescence Switching. A pronounced concentration-dependent fluorescence switching was observed in **R3** (Figure 7). Such a striking behavior was not shown by other compounds studied. A dilute solution of **R3** (4.10×10^{-9} M in dichloromethane) emits blue ($\lambda_{\max} \sim 430$ nm). However, the emission shows a red-shift and becomes structureless at higher concentrations. The latter emission can be assigned to the excimer state. The emission becomes green and the intensity keeps increasing in the concentration range of

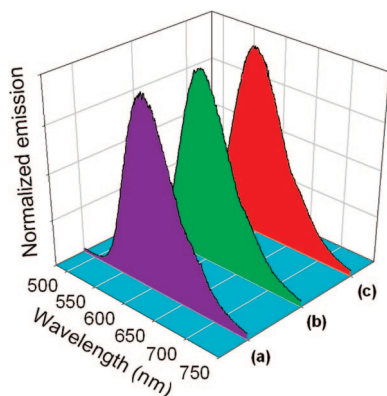


FIGURE 8. Emission spectra recorded from thin films of **R2**: (a) pristine, (b) after exposing the film for more than 4 weeks at ambient condition, and (c) after heating at 150 °C for 24 h and cooling to room temperature.

10^{-6} to 10^{-5} M. In fact, the emission was green ($\lambda_{\text{max}} \sim 475$ nm) at a concentration as high as 2.60×10^{-4} M, but severe quenching of fluorescence was observed when the concentration was further increased. For example, the emission intensity was negligible at a concentration of 5.30×10^{-3} M. This indicates that the excimer emission is facilitated by an increase in concentration to a certain extent. Since the solution emission of **R3** originates from the $\pi-\pi^*$ state, a large increase in concentration quenches such an excited state.

Interestingly, the fluorescence of this compound was not quenched in the solid state, even though the molecules are closer than in solution. **R3** contains an elongated, flat side chain comprised of multiple ethynylphenyl groups. As its concentration is increased, molecules of **R3** come in close proximity forming stacked structures even in solution. This explains why the compound exhibits significantly red-shifted emission in concentrated solution and in the solid state (120 nm). Although fluorescence was severely quenched at higher concentrations in solution, the ϕ_{F} measured in the solid state (0.25) was similar to that recorded in dichloromethane ($\phi_{\text{F}} = 0.30$) at a lower concentration. This again indicates that the solid-state emission of **R3** originates from the ICT state. An emission from the ICT state should not be quenched by the stacking of the molecules. A $\pi-\pi$ interaction would rather facilitate the formation of the ICT state.

Effect of Aging and Annealing. Thin films of **B1–R3** were exposed to ambient light for several weeks, as well as being heated to 150 °C for 24 h. There was no change in the emission spectra before and after either treatment. For example, the fluorescence spectra of thin films of **R2** recorded under different conditions (pristine, after exposing the film for several weeks, and after heating the film at 150 °C for 24 h) are essentially the same (Figure 8). Compounds **B1–R3** maintain their color purity and are reasonably stable under the conditions used for aging and annealing.

Temperature-Dependent Emission. We also studied the effect of temperature on the absorption and emission spectra of **B1**, **B3**, **G2**, and **G3**. There is no change in the absorption spectra, but these compounds show a small red-shift in the emission with decreasing temperature (Figure 9). For example, the emission of **B1** recorded at -10 °C ($\lambda_{\text{max}} = 420$ nm) is about 14 nm red-shifted from that at 25 °C ($\lambda_{\text{max}} = 406$ nm) (Table 3) likely because alignment of the solvent dipole around the molecule in the excited state is prevented at low temperature. A change in the dielectric constant of the solvent upon cooling

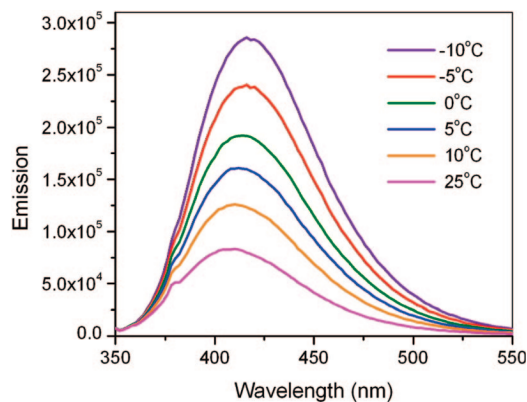


FIGURE 9. Emission spectra of **B1** recorded at different temperatures.

TABLE 3. Emission maxima (λ_{max}) and Fluorescence Quantum Yields (ϕ_{F}) of **B1** and **G3** Recorded at Different Temperatures^a

temp (°C)	B1		G3	
	λ_{max} (nm)	ϕ_{F} (nm)	λ_{max} (nm)	ϕ_{F} (nm)
25	406	0.05	453	0.07
10	412	0.10	454	0.15
5	414	0.12	456	0.17
0	414	0.15	456	0.19
-5	416	0.18	456	0.21
-10	420	0.20	458	0.25

^a Excitation wavelength for **B1** ($\lambda_{\text{ex}} = 330$ nm) and **G3** ($\lambda_{\text{ex}} = 360$ nm); error in the ϕ_{F} values = ± 0.01 .

may be important. The ϕ_{F} values increase nominally but systematically as the temperature is decreased (Table 3). The ϕ_{F} values of **B1** (0.05) and **G3** (0.07) at 25 °C, for example, are lower than those measured at -10 °C (0.20 and 0.25, respectively). The rotational deactivations of the singlet excited states are minimized at lower temperatures, resulting in an increase in the fluorescence quantum yield.

Conclusions

A photophysical study of stable blue, green, and orange-red light-emitting carbazoles (**B1–B3**, **G1–G3**, and **R1–R3**) was carried out. The solid-state emission was red-shifted from the solution (dichloromethane) emission for each compound, except for **R1** which showed an unusual blue-shift. The substitution pattern on the carbazole significantly affected the relative red-shift of the corresponding solution spectra and that observed in the solid state. For example, the red-shifts in the solid state of **B1–B3** and **G1–G3** are in the range of ~ 15 and ~ 30 nm, respectively, but as high as 120 nm for **R3**. The ϕ_{F} values of **B2** and **R1–R3** were found to be decent both in solution (0.30–0.52 in dichloromethane) and in the solid state (0.21–0.45). However, the ϕ_{F} values of **B1**, **B3**, **G1–G3**, and **R1–R3** were extremely low (0.03–0.15), indicating that the EW groups such as the carbaldehyde and malononitrile groups effectively quench the fluorescence. The τ_{F} values, on the other hand, were not found to be affected by the substitution pattern. The singlet states of the compounds having EW groups are more polar than their corresponding ground states. This results in **B1**, **B3**, and **G1–G3** exhibiting positive solvatochromism and **B2** showing negligible solvatochromism. Such a systematic solvatochromism was not exhibited by **R1–R3** because of the twisted ICT nature of their singlet states. Lowering the temperature from 25 to -10 °C

caused a small but distinct red-shift in the emissions and a slight increase in the ϕ_F values of **B1**, **B3**, **G2**, and **G3**. When the thin films containing **B1–R3** were exposed to ambient conditions for at least 4 weeks or heated at 150 °C for 24 h, the emission purity was retained, indicating that these are robust compounds.

Experimental Section

Fluorescence Quantum Yields (ϕ_F). The ϕ_F values in solution were measured following a general method with 9,10-diphenylanthracene ($\phi_F = 0.9$ in cyclohexane) and riboflavin (0.3 in ethanol) as the standard.³² Dilute solutions of these compounds in appropriate solvents were used. Sample solutions were in quartz cuvettes were degassed for ~15 min. The degassed solutions had absorbances of 0.05–0.09 at absorbance maxima. The fluorescence spectra of each were recorded 3–4 times, and an average value of integrated areas of fluorescence was used for the calculation of ϕ_F in solution. The refractive indices of solvents at the sodium D line were used. The ϕ_F values in the solid state were measured following a literature method.^{37–39} A concentrated dichloromethane solution of sample was cast as a thin film on a quartz plate and then allowed to dry. The plate was inserted into an integrating sphere, and the required spectra were recorded. The samples were excited at absorption maxima in dichloromethane. It is well-known that for compounds showing an overlap of the absorption and the emission spectra (a small Stokes shift), the use of an integrating sphere results in a substantial loss of emission due to reabsorption of the emitted light. A method employed earlier was used to minimize the impact of this on the calculation of the ϕ_F .³⁷

Fluorescence Lifetime (τ_F) Measurements. Solutions with an absorbance of 0.1–0.25 at the absorption maxima were placed in quartz cuvettes. Fluorescence decay profiles of argon-degassed (~15 min) solutions were recorded with the use of a single photon counting spectrofluorimeter. Decays were monitored at the corresponding emission maxima of the compounds. In-built software allowed the fitting of the decay spectra ($\chi^2 = 1–1.5$) and yielded the fluorescence lifetimes.

Synthesis. Compounds **B1–B3** and **G1–G3** were synthesized starting from carbazole. The synthesis of **R1–R3** is provided elsewhere.²⁶

9-(Phenanthren-9-yl)-9H-carbazole (3). Carbazole (30 mmol), 9-bromophenanthrene (60 mmol), potassium carbonate (200 mmol), and nitromethane (200 mL) were mixed in a dry round-bottom flask and refluxed for 2 days. Solvent was distilled off, and the product was purified by column chromatography (silica gel, dichloromethane/hexanes (1:5)), affording pure **3** as a white solid (yield 70%). ¹H NMR (300 MHz, CDCl₃): δ 7.16 (d, 2H), 7.39 (m, 6H), 7.71 (m, 1H), 7.80 (m, 1H), 7.90 (d, 1H), 8.01 (s, 2H), 8.30 (d, 2H), 8.90 (t, 2H). ¹³C NMR (300 MHz, CDCl₃): δ 110.2, 119.7, 120.3, 122.8, 123.2, 124.1, 126.0, 127.2, 127.3, 127.5, 127.6, 127.8, 129.0, 129.5, 130.6, 131.8, 132.6, and 142.5. MS (EI) calculated for C₂₆H₁₇N 343.1334, measured 343.1364.

3,6-Dibromo-9-(naphthalen-1-yl)-9H-carbazole (4). 9-(Naphthalen-1-yl)-9H-carbazole (12 mmol) in 100 mL of glacial acetic acid was subjected to sonication for 20 min and then stirred for 30 min in a round-bottom flask. Bromine (6 mmol) in 20 mL of glacial acetic acid was slowly added into the mixture over 20 min while stirring at room temperature. The mixture was stirred for an additional 20 min at the same temperature. Ice cold water (100 mL) was then added. The mixture was then subjected to suction filtration. The residue was washed several times with water and was then dried over vacuum to get pure **4** (yield 95%). ¹H NMR

(300 MHz, CDCl₃): δ 6.88 (d, 2H), 7.15 (d, 1H), 7.35 (d, 1H), 7.44 (d, 2H), 7.60 (m, 2H), 7.68 (d, 1H), 8.08 (m, 2H), 8.30 (s, 2H). ¹³C NMR (300 MHz, CDCl₃): δ 112.5, 113.3, 123.0, 123.5, 124.0, 126.0, 126.5, 127.0, 127.5, 128.5, 129.5, 130.5, 133.0, 135.0, and 141.5. MS (EI) calculated for C₂₂H₁₃Br₂N 448.9415, measured 448.9449.

3,6-Dibromo-9-(phenanthren-9-yl)-9H-carbazole (5). Compound **3** (20 mmol) was mixed with acetic acid in a round-bottom flask and subjected to sonication followed by stirring for 30 min. Into this mixture was slowly dropped bromine (10 mmol) in 30 mL of glacial acetic acid (30 min) with stirring. After 2 h of additional stirring, ice-cold water was poured in. The mixture was subjected to suction filtration. The residue was washed with water several times to obtain **5** in the form of a yellowish white compound, which was dried under vacuum (yield 95%). ¹H NMR (300 MHz, CDCl₃): δ 6.91 (d, 2H), 7.11 (d, 1H), 7.41 (m, 3H), 7.70 (d, 2H), 7.79 (d, 1H), 8.29 (s, 2H), 8.80 (s, 2H). ¹³C NMR (300 MHz, CDCl₃): δ 112.0, 113.0, 122.8, 123.3, 123.7, 123.9, 127.4, 127.8, 127.9, 128.0, 129.0, 129.1, 129.5, 130.8, 131.4, 131.6, 131.8, and 141.0. MS (EI) calculated for C₂₆H₁₅Br₂N 498.9571, measured 498.9606.

3,6-Diiodo-9-(phenanthren-9-yl)-9H-carbazole (6). Compound **3** (5 mmol) was dissolved in dichloromethane (100 mL). A solution of *N*-iodosuccinimide (11 mmol) in dichloromethane (10 mL) was slowly added to it. The whole mixture was stirred in the dark for 6 h at room temperature. The solvent was evaporated to get **6** (yield 90%). ¹H NMR (300 MHz, CDCl₃): δ 6.81 (d, 2H), 7.11 (d, 1H), 7.40 (m, 1H), 7.58 (d, 2H), 7.69 (m, 2H), 7.78 (m, 1H), 7.84 (s, 2H), 8.45 (s, 2H), 8.81 (s, 2H). ¹³C NMR (300 MHz, CDCl₃): δ 82.0, 112.0, 122.8, 123.2, 123.5, 124.2, 127.3, 127.38, 127.6, 127.7, 128.0, 129.0, 129.1, 129.6, 130.6, 131.3, 131.5, 131.8, 135.0, and 141.0. MS (EI) calculated for C₂₆H₁₅I₂N 594.9294, measured 594.9302.

9-(Phenanthren-9-yl)-9H-carbazole-3-carbaldehyde (B1). Compound **5** (4 mmol) in dry tetrahydrofuran (60 mL) was stirred under argon and cooled to –78 °C. *n*-Butyl lithium (8 mmol in pentane) was slowly added with vigorous stirring. Stirring was continued for two hours at the same temperature. Dry dimethylformamide (25 mmol) was added and the mixture allowed stirring for two more hours at the same temperature. It was mixed with 2N hydrochloric acid at room temperature, extracted with ether, and purified by chromatography (silica gel, dichloromethane/hexanes (1:5)) to get pure **B1** (yield-30%). ¹H NMR (300 MHz, CDCl₃): δ 7.10 (m, 2H), 7.2 (s, 1H), 7.40 (m, 3H), 7.70 (m, 2H), 7.80–8.02 (m, 4H), 8.32 (m, 1H), 8.75 (s, 1H), 8.84 (m, 2H), 10.15 (s, 1H). ¹³C NMR (300 MHz, CDCl₃): δ 110.5, 111.0, 120.8, 121.3, 122.8, 123.0, 123.3, 123.6, 123.8, 127.0, 127.2, 127.5, 127.8, 128.0, 129.0, 129.5, 130.5, 131.5, 131.8, 131.9, 142.0, 145.0, and 191.0. MS (EI) calculated for C₂₇H₁₇NO 371.1310, measured 371.1309.

9-(Phenanthren-9-yl)-3,6-bis(2-phenylethynyl)-9H-carbazole (B2). Compound **6** (3 mmol), *trans*-dichlorobis(triphenylphosphine)palladium(II), diisopropylamine (50 mL), phenylacetylene (6.2 mmol), benzene (10 mL), copper iodide (0.1 mmol), and triphenyl phosphine (0.3 mmol) were added in a dry round-bottom flask. The mixture was refluxed for 12 h. The solvent was evaporated, and the solid obtained was subjected to column chromatography (silica gel, dichloromethane/hexanes (1:9)). The fraction containing **B2** was evaporated to obtain pure **B2** as white powder (yield 56%). ¹H NMR (300 MHz, CDCl₃): δ 7.05 (d, 2H), 7.28 (s, 1H), 7.35–7.45 (m, 6H), 7.47 (d, 1H), 7.54–7.65 (m, 6H), 7.75 (m, 2H), 7.85 (t, 1H), 8.00 (s, 2H), 8.45 (s, 2H), 8.90 (t, 2H). ¹³C NMR (300 MHz, CDCl₃): δ 88.0, 90.0, 111.0, 115.0, 122.8, 123.2, 123.5, 123.8, 124.2, 127.3, 127.5, 127.7, 128.0, 128.4, 129.0, 129.1, 130.0, 130.5, 131.5, and 131.7. MS (EI) calculated for C₄₂H₂₅N 543.1987, measured 543.1998.

4,4'-Bis((9H-carbazol-9-yl)-3,3'-dicarbaldehyde)biphenyl (B3). Phosphoryl chloride (0.1 mol) was added dropwise into cooled *N,N*-dimethylformamide (DMF, 0.1 mol) in an ice bath. The mixture was maintained at room temperature for 1 h, and a solution of **8**

(37) Shah, B. K.; Neckers, D. C.; Shi, J.; Forsythe, E. W.; Morton, D. *Chem. Mater.* **2006**, *18*, 603.

(38) de Mello, J. C.; Wittmann, H. F.; Friend, R. H. *Adv. Mater.* **1997**, *9*, 230.

(39) Palsson, L. O.; Monkman, A. P. *Adv. Mater.* **2002**, *14*, 757.

(0.004) in 5 mL of DMF was added. The reaction mixture was heated at 130 °C with stirring for 24 h and then poured into cracked ice. After neutralizing with a base, the mixture was extracted with chloroform. The extract phase was dried with anhydrous magnesium sulfate, and the solvent was removed by distillation in a vacuum. The solid residue was purified by using silica gel column chromatography (ethyl acetate/hexanes (1:4)) to obtain a whitish-yellow solid (yield 50%). ¹H NMR (300 MHz, CDCl₃): δ 7.40 (m, 2H), 7.50–7.60 (m, 6H), 7.75 (d, 4H), 8.01 (m, 6H), 8.25 (d, 2H), 8.70 (s, 2H), 10.10 (s, 2H). ¹³C NMR (300 MHz, CDCl₃): δ 110.0, 110.3, 121.1, 121.5, 123.3, 124.7, 125.0, 127.0, 127.5, 128.0, 129.0, 129.7, 136.5, 140.0, 142.0, 144.5, and 192.0. MS (EI) calculated for C₃₈H₂₄N₂O₂ 540.1838, measured 540.1853.

9-(Naphthalen-1-yl)-9H-carbazole-3-carbaldehyde (9). This compound was obtained as a side product while synthesizing **13** (see below). It was obtained in 30% yield as white powder and dried under vacuum. ¹H NMR (300 MHz, CDCl₃): δ 7.04 (d, 2H), 7.20 (d, 1H), 7.35–7.47 (m, 3H), 7.55 (d, 1H), 7.65 (m, 2H), 7.90 (d, 1H), 8.10 (dd, 2H), 8.28 (d, 1H), 8.80 (s, 1H), 10.15 (s, 1H). ¹³C NMR (300 MHz, CDCl₃): δ 110.5, 111.0, 120.5, 121.0, 123.0, 123.3, 123.5, 123.8, 125.8, 126.8, 127.3, 127.6, 127.8, 128.5, 129.5, 129.8, 130.5, 133.0, 135.0, 143.0, 146.0, 192.0. MS (EI) calculated for C₂₃H₁₅NO 321.1154, measured 321.1136.

9-(Naphthalen-1-yl)-9H-carbazole-3,6-dicarbaldehyde (10). This compound was synthesized in a different way than the reported method.⁴⁰ Compound **4** (10 mmol) was dissolved in dry tetrahydrofuran in a dry two-necked round-bottom flask that was charged with argon and cooled in an acetone–dry ice bath. *tert*-Butyllithium in pentane (20 mmol) was added slowly with vigorous stirring. The mixture was stirred for an additional 2 h at the same temperature. Dry dimethylformamide (25 mmol) was added, and the mixture was stirred for an additional 2 h at the same temperature. It was subsequently mixed with 2 N hydrochloric acid at room temperature, extracted with ether, and purified by chromatography (silica, dichloromethane/hexanes (1:5)). Compound **13** was obtained as white powder (yield 40%). It was dried under vacuum before characterization. ¹H NMR (300 MHz, CDCl₃): δ 7.10 (m, 3H), 7.38 (d, 1H), 7.55–7.70 (m, 3H), 7.95 (d, 2H), 8.05 (d, 1H), 8.15 (d, 1H), 8.80 (s, 2H), 10.20 (s, 2H). ¹³C NMR (300 MHz, CDCl₃): δ 111.0, 122.5, 123.5, 124.0, 126.0, 126.5, 127.3, 127.8, 128.5, 129.0, 130.5, 130.7, 132.0, 135.0, 147.0, and 192.0. MS (EI) calculated for C₂₄H₁₅NO₂ 349.1103, measured 349.1106.

2-((9-(Phenanthren-9-yl)-9H-carbazol-3-yl)methylene)malononitrile (G1). Compound **B1** (4 mmol), malononitrile (4.2 mmol), basic aluminum oxide (20 mmol), and toluene (100 mL) were added to a round-bottom flask. The mixture was refluxed for 6 h, cooled to room temperature, and filtered, and the residue was washed with dichloromethane. The filtrate was evaporated, and the

solid obtained was purified by chromatography (silica, dichloromethane/hexanes (1:4)). The procedure afforded pure **G1** as yellow powder (yield 80%). ¹H NMR (300 MHz, CDCl₃): δ 7.10–7.20 (m, 3H), 7.40–7.48 (m, 3H), 7.55 (m, 2H), 7.80–7.98 (m, 5H), 8.30 (dd, 1H), 8.85 (m, 3H). ¹³C NMR (300 MHz, CDCl₃): δ 111.1, 113.3, 114.0, 115.0, 120.8, 121.7, 122.5, 122.7, 123.5, 123.6, 124.3, 124.8, 127.5, 127.5, 127.6, 127.7, 127.7, 127.8, 128.3, 128.8, 129.1, 129.3, 130.8, 131.2, 131.4, 131.9, 143.0, 145.0, and 160.0. MS (EI) calculated for C₃₀H₁₇N₃ 419.1422, measured 419.1436.

2-((9-(Naphthalen-1-yl)-9H-carbazol-3-yl)methylene)malononitrile (G2). The same synthetic procedure employed for **G1** was used to prepare **G2**. Compound **12** (4 mmol) was used instead of **B1**. The procedure afforded pure **G2** as yellow powder (yield 80%). ¹H NMR (300 MHz, CDCl₃): δ 7.05 (d, 1H), 7.20 (d, 1H), 7.40 (m, 3H), 7.55–7.7 (m, 4H), 7.92 (m, 2H), 8.05 (d, 1H), 8.13 (d, 1H), 8.28 (d, 1H), 8.82 (s, 1H). ¹³C NMR (300 MHz, CDCl₃): δ 111.0, 111.2, 121.0, 121.8, 122.6, 123.4, 124.1, 124.8, 126.0, 126.5, 127.1, 127.8, 127.9, 128.8, 129.0, 130.0, 130.3, 132.4, 135.0, 143.0, 145.0, and 160.0. MS (EI) calculated for C₂₆H₁₅N₃ 369.1266, measured 369.1266.

2,2'-(9-(Naphthalen-1-yl)-9H-carbazol-3,3'-yl)methylene)malononitrile (G3). This compound was prepared using the synthetic procedure also used for the preparation of **G1**. Compound **13** (4 mmol) was used instead of **B1**. Double the amount of malononitrile (8.4 mmol) was used. Compound **G3** was obtained as yellow powder (yield 80%). ¹H NMR (300 MHz, CDCl₃): δ 7.10 (d, 1H), 7.15 (d, 2H), 7.40 (t, 1H), 7.62 (m, 2H), 7.72 (t, 1H), 7.95 (s, 2H), 8.08 (d, 3H), 8.19 (s, 1H), 8.80 (s, 2H). ¹³C NMR (300 MHz, CDCl₃): δ 80.0, 112.3, 113.4, 114.3, 122.0, 123.5, 124.7, 125.3, 125.9, 126.5, 127.4, 128.1, 129.0, 129.7, 130.8, 131.2, 135.0, 146.0, and 160.0. MS (EI) calculated for C₃₀H₁₅N₅ 445.1327, measured 445.1332.

Acknowledgment. We thank Dr. T. H. Kinstle for valuable suggestions concerning synthesis and Dr. Rajib Mondal for fruitful discussions about photophysical measurements. Financial support from the Research Corporation for Science Advancement (Cottrell College Science Award to BKS) is highly appreciated. This work was partly supported by the Endowment Fund of the Center for Photochemical Sciences. We thank the donors of these funds.

Supporting Information Available: Absorption and emission spectra of **B2**, **G2**, and **R2**, fluorescence decay profiles, geometry optimized structures, and NMR spectra of **B1–B3**, **G1–G3**, and **R1–R3**. This material is available free of charge via the Internet at <http://pubs.acs.org>.

(40) Feng, L.; Zhang, C.; Chen, Z.; Qin, A.; Yuan, M.; Bai, F. *J. Appl. Polym. Sci.* **2006**, *100*, 923.